Feasibility of Contrast-Enhanced CT with Knowledge-Based Iterative Model Reconstruction Algorithm for the Evaluation of Parotid Gland Masses

Kiwook Kim

Department of Medicine

The Graduate School, Yonsei University

Feasibility of Contrast-Enhanced CT with Knowledge-Based Iterative Model Reconstruction Algorithm for the Evaluation of Parotid Gland Masses

The Master's Thesis
submitted to the Department of Medicine
the Graduate School of Yonsei University
in partial fulfillment of the requirements for the degree of
Master of Medical Science

Kiwook Kim

June 2016

This certifies that the Master's Thesis of

Kiwook Kim is approved.

Thesis Supervisor : Jinna Kim

Thesis Committee Member#1 : Sang-Sun Han

Thesis Committee Member#2 : Yoon Woo Koh

The Graduate School
Yonsei University

June 2016

ACKNOWLEDGEMENTS

I wish to acknowledge my special thanks to Professor Jinna Kim, who is my thesis director, for supporting my efforts with total commitment and facilitating every step of the process. Until the completion of the final draft, she gave me shared with me her constructive and practical insights. No words can express my thanks for her efforts on my behalf.

I am also indebted to Professor Yoon Woo Koh and Sang-Sun Han, for their help for pertinent advice to assure the superior quality of this paper.

Additionally, I express gratitude to my family for their support and encouragement.

<TABLE OF CONTENTS>

LIST OF FIGURES

LIST OF TABLES

ABSTRACT

Feasibility of Contrast-Enhanced CT with Knowledge-Based Iterative Model Reconstruction Algorithm for the Evaluation of Parotid Gland Masses

Kiwook Kim

Department of Medicine
The Graduate School, Yonsei University

Purpose: The purpose of this study was to assess the diagnostic utility of knowledge-based iterative model reconstruction (IMR) algorithm for CT evaluation of parotid gland masses and compare the finding with those of filtered back projection (FBP) and hybrid iterative reconstruction (iDose^4) using the same CT datasets.

Materials and methods: Forty-two consecutive patients with palpable parotid masses who underwent contrast-enhanced CT were enrolled. The same data were reconstructed using FBP, iDose^4, and knowledge-based IMR algorithms. Quantitative imaging parameters, including background noise, signal-to-noise ratio (SNR), and contrast-to-noise ratio (CNR), were measured. Subjective assessment for noise and artifact, parotid mass delineation, and blotchy, pixelated appearance was also performed by two independent radiologists using a five-point grading system.

Results: The background noise was significantly lower with the IMR algorithm than with the other two algorithms (p<0.001), while the SNR and CNR were significantly higher with the former than with the latter (p<0.001). The IMR algorithms resulted in significantly lesser noise and

artifacts (p<0.001) and better image quality for parotid mass delineation (p<0.001) compared with the other two algorithms, although it was assoctiated more frequently with a blotchy, pixelated appearance that would not or slightly affect the diagnosis ($p < 0.001$).

Conclusion: CT with knowledge-based IMR provides excellent image quality and decreases image noise and artifacts. Therefore, it can be considered clinically feasible for the assessment of parotid gland mass.

Keywords: knowledge-based iterative reconstruction, filtered back projection, computed tomography, parotid gland mass

Feasibility of Contrast-Enhanced CT with Knowledge-Based Iterative Model Reconstruction Algorithm for the Evaluation of Parotid Gland Masses

Kiwook Kim

Department of Medicine
The Graduate School, Yonsei University

I. INTRODUCTION

Parotid gland tumors account for approximately 3% of all head and neck tumors[1], with a majority of patients presenting with a palpable mass in the preauricular region.

For patients with suspected parotid gland tumors, computed tomography (CT) can easily confirm the presence of parotid mass, determine whether the tumor is benign or aggressive, and assess the extent. This can guide the next step of management and aid in appropriate treatment selection. However, streak artifacts caused by dental amalgam restorations on CT often interfere with the evaluation of the parotid gland and Stenson duct; furthermore, they increase the difficulty of evaluating masses arising from the deep lobe of the gland, which lies anterior to the styloid process of the temporal bone and lateral to the parapharyngeal fat [2].

Ongoing research has continued to improve the quality of CT images, and there is a noticeable progression in CT reconstruction algorithms, particularly iterative

reconstruction (IR) techniques[3]. The most recently introduced knowledge-based iterative model reconstruction (IMR) system (Philips Healthcare, Cleveland, OH, USA) has been applied for CT imaging of various body parts and has shown several advantages compared with previous CT reconstruction algorithms, such as better image quality and decreased noise and radiation dose [4-7].

The purpose of this study was to assess the diagnostic utility of IMR for CT evaluation of patients with parotid gland masses and compared the finding with those of other reconstruction algorithms.

II. MATERIALS AND METHODS

1. Patients

This prospective clinical study was approved by our Institutional Review Board, and informed consent was obtained from each patient. Between April and December 2015, 42 consecutive patients (16 men and 26 women) with suspected parotid gland tumors who were scheduled to undergo contrast-enhanced CT were enrolled in this study. The median patient age was 50.5 years (range, 20-78 years), and the median body mass index (BMI) was 23.4 kg/m2 (range, 18.9-35.3 kg/m2).

Of the total, 36 patients underwent surgical excision or biopsy for their parotid gland masses, and the final histopathological diagnoses were benign non-neoplastic lesion in two, benign neoplasm in 28, and malignancy in six. The specific histological types included lymphoepithelial cyst (n = 1), branchial cleft cyst (n = 1), pleomorphic adenoma (n = 23), Warthin tumor (n = 3), basal cell adenoma (n = 1), myoepithelioma (n = 1), mucoepidermoid carcinoma (n = 1), salivary duct carcinoma (n = 1) and lymphoma (n = 4). The remaining six patients were

diagnosed with acute parotitis (n=3), pneumoparotid (n=1), and lipoma (n=2) on the basis of the imaging findings and did not undergo any further diagnostic or therapeutic procedures. The mean size of the 38 measurable masses on CT images was 22.6 ± 9.6 mm (range, 8.1-51.0 mm).

2. Image acquisition and reconstruction

All studies were performed using a 256-row multidetector CT (Brilliance iCT scanner; Philips Healthcare, Cleveland, OH, USA) at our institution. CT images were acquired at a manually fixed peak tube voltage of 100kVp, with automated Z-axis dose modulation using a scout image (DoseRight; Philips Healthcare, Cleveland, OH, USA). The maximal tube current was limited to 150 mAs, and the effective mAs ranged from 77 to 131 mAs. The field of view was 180 mm, with a matrix of 512 × 512. The other scanning parameters were as follows: detector configuration, 128 × 0.625 mm; pitch, 0.601; tube rotation time, 0.5 s; and acquisition mode, helical.

All patients underwent contrast-enhanced CT in the supine position using a standard CT protocol for the neck. Contiguous images of the neck were acquired in the axial plane from the orbital floor to the suprasternal notch. A total of 80-100 mL of the iodinated contrast medium Iobitridol (Xenetix 300; Guerbet, Roissy, France) was intravenously administered at a flow rate of 2 mL/s using an automated injector, followed by the injection of 40 mL of 0.9 % saline solution at the same flow rate. Contrast-enhanced CT scans were obtained at 40–60 s after the initiation of contrast agent administration.

Three axial image datasets were created by reconstructing the identical raw projection dataset using three different algorithms, namely FBP, iDose^4 level 3

(which is a fourth-generation hybrid iterative reconstruction algorithm supplied by Philips Healthcare), and IMR level 1. The iDose[4] and IMR algorithms include levels 1-7 and levels 1-3, respectively, with a higher level providing greater noise reduction. All reconstructed section thicknesses were 3 mm.

To evaluate the radiation dose, the CT dose index volume (CTDIvol, described in mGy) and dose length product (DLP, described in mGy-cm) were recorded, according to the dose report [8].

3. Objective image analysis

For objective image assessments, the background noise (BN), signal-to-noise ratio (SNR), and contrast-to-noise ratio (CNR) were measured as quantitative image parameters on a Picture Archiving and Communication System (PACS) workstation (Centricity RA 1000; GE Healthcare, USA). A head and neck radiologist with 6 years of experience recorded the averaged attenuation values (V) and standard deviation (SD) of Hounsfield units (HU) by placing a circular or ovoid region of interest (ROI) measuring approximately 10 mm in diameter in the two empty spaces on both sides of the head (air), masseter muscle (MM), and internal jugular vein (IJV) at the same level of the parotid gland mass (Fig 1). The measurement was repeatedly obtained for each of the three image datasets, and BN, SNR, and CNR were calculated by applying the following formula:

$$\mathrm{BN} = \frac{SD_{Air\ right} + SD_{Air\ left}}{2} \qquad \mathrm{SNR} = \frac{V_{MM}}{\mathrm{BN}} \qquad \mathrm{CNR} = \frac{|V_{MM} - V_{IJV}|}{\sqrt{{SD_{MM}}^2 + {SD_{IJV}}^2}}$$

Figure 1. Assessment of objective image quality at the level of the parotid gland. Region of interests drawn to bilaterally measure the standard deviation of air (background noise) and attenuation of the masseter muscle and internal jugular vein for the estimation of the signal-to-noise ratio and contrast-to-noise ratio.

4. Subjective image analysis

Two radiologists with 15 and 4 years of experience, respectively, independently assessed three axial image sets displayed on three monitors at the same time using a PACS workstation. In addition to the default preselected window settings (window

width of 350 HU, window level of 60 HU), the radiologists were allowed to change the window width and level for optimal viewing conditions. Images were shown in a random manner, not in a side-by-side manner. Both radiologists were blinded to the patient data, clinical information, and image reconstruction technique.

For each image dataset, each radiologist graded image noise and artifacts (1 = significant, 2 = moderate, 3 = mild, 4 = minimal, 5 = no), delineation of the parotid mass (1 = nondiagnostic, 2 = over-smoothening, 3 = acceptable, 4 = good, 5 = excellent), and a blotchy, pixelated appearance (1 = severely affecting the diagnosis, 2 = moderately affecting the diagnosis, 3 = slightly affecting the diagnosis, 4 = not affecting the diagnosis, 5 = no blotchy, pixelated appearance) using a five-point grading system [9].

5. Statistical analysis

All statistical analyses were performed using SPSS version 20.0 (SPSS Inc., Chicago, IL, USA). All recorded data are presented as means ± SDs. Quantitative imaging parameters (BN, SNR, and CNR) for the three reconstruction algorithms were compared using one-way repeated analysis of variance (ANOVA) followed by Bonferroni post hoc tests. Subjective image quality scores were analyzed using Friedman tests, followed by Wilcoxon signed-rank tests. Interobserver agreement for the subjective image analyses was calculated using Cohen's kappa statistics with quadratic weighting, and estimation of the overall kappa was based on the study of Landis and Koch[10] as follows: slight agreement (0-0.20), fair agreement (0.21-0.40), moderate agreement (0.41-0.60), substantial agreement (0.61-0.80), and almost perfect agreement (0.81-1.00). A p-value of <0.05 was considered statistically significant.

III. RESULTS

The results of the objective image analyses are summarized in Table 1. The mean BN value was significantly lower with the IMR algorithm than with the FBP and iDose^4 algorithms ($p<0.001$ for all pairs). The mean SNR and CNR values were significanty higher with the IMR algorithm than with the FBP ($p<0.001$ for both) and iDose^4 algorithms ($p<0.001$ for both), although there was no significant difference in the SNR value for the masseter muscle between the FBP and iDose^4 algorithms ($p=0.06$).

The results of subjective image analyses are shown in Table 2. The IMR algorithm was significantly better than the FBP and iDose^4 algorithms with regard to noise and artifact reduction ($p<0.01$ for all pairs for both readers) and delineation of the parotid mass ($p<0.01$ for all pairs for both readers; Fig 2). However, the score for a blotchy, pixelated appearance was significantly lower for the IMR algorithm than for the FBP and iDose^4 algorithms ($p<0.01$ for all pairs for both readers), which indicated that the IMR algorithm was more often associated with a blotchy, pixelated appearance compared with the other two algorithms (Fig 3).

Interobserver agreements for the subjective image analyses were moderate to substantial for all parameters (noise and artifacts: $\kappa=0.67$, delineation of the parotid mass: $\kappa=0.58$, and a blotchy, pixelated appearance: $\kappa=0.57$).

The average CTDIvol and DLP were 3.78 ± 0.94 mGy and 149.22 ± 40.69 mGy-cm, respectively.

Table 1. Result of the objective analysis of reconstruction techniques.

Parameters	Reconstruction techniques			Comparison (p value)		
	FBP	iDose^4	IMR	FBP vs. iDose^4	iDose^4 vs. IMR	IMR vs. FBP
Background noise	11.38±3.69	8.50±3.49	3.98±3.38	0.001	<0.001	<0.001
SNR[1]	7.28±1.85	10.09±2.97	24.04±6.75	0.012	<0.001	<0.001
CNR[2]	5.78±2.09	11.28±4.63	17.64±8.25	<0.001	<0.001	<0.001

[1]: SNR measured at the masseter muscle.

[2]: CNR between the masseter muscle and internal jugular vein.

SNR : Signal to noise ratio, CNR : Contrast to noise ratio, FBP : filtered back projection, iDose^4 : hybrid iterative reconstruction, IMR : knowledge-based iterative model reconstruction.

Table 2. Result of the subjective analysis of reconstruction techniques

Parameters	Reader	Reconstruction techniques			Comparison (p value)		
		FBP	iDose4	IMR	FBP vs. iDose^4	iDose^4 vs. IMR	IMR vs. FBP
Noise & artifact	R1	2.69±0.87	3.40±0.96	4.19±0.86	<0.001	<0.001	<0.001
	R2	2.62±0.94	3.55±0.86	4.40±0.66	<0.001	<0.001	<0.001
Delineation of the parotid mass	R1	3.14±1.20	3.83±1.15	4.43±0.80	<0.001	<0.001	<0.001
	R2	3.50±1.02	4.02±0.90	4.60±0.66	<0.001	<0.001	<0.001
Blotchy pixelated appearance	R1	4.88±0.33	4.64±0.58	3.76±0.76	0.004	<0.001	<0.001
	R2	4.93±0.26	4.48±0.59	4.02±0.68	<0.001	<0.001	<0.001

FBP : filtered back projection, iDose^4 : hybrid iterative reconstruction, IMR : knowledge-based iterative model reconstruction.

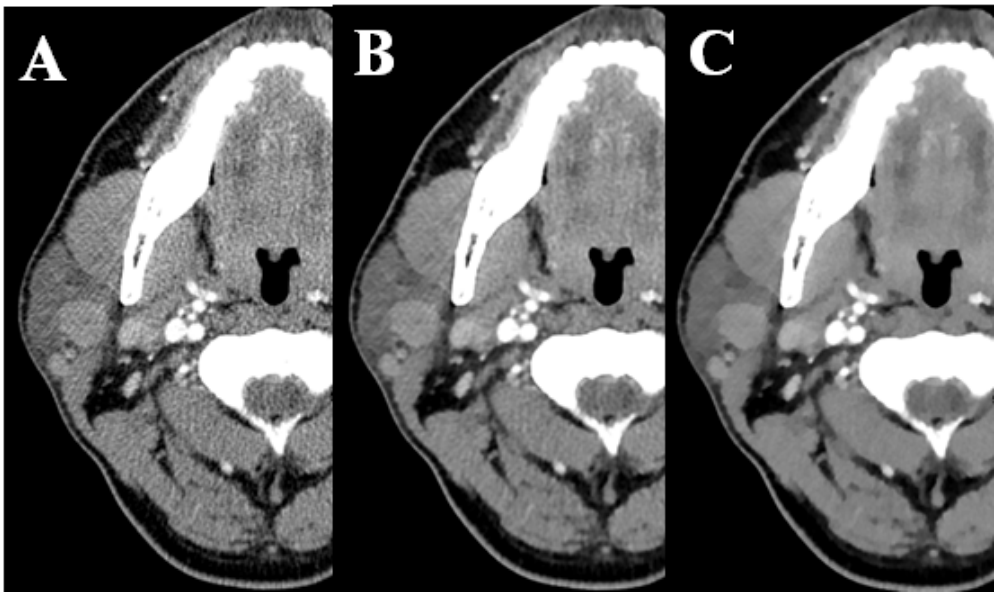

Figure 2. 63-year-old woman with a right parotid gland mass.

Three axial image sets reconstructed using filtered back projection (FBP) (A), hybrid iterative reconstruction (iDose^4) (B), and knowledge-based iterative model reconstruction (IMR) (C) algorithms. Compared with those on the FBP- and iDose^4-reconstructed images, there is a significant decrease in the streak artifacts related to dental amalgam in the parotid area and better conspicuity and definition of the tumor margins on the iterative model-reconstructed image.

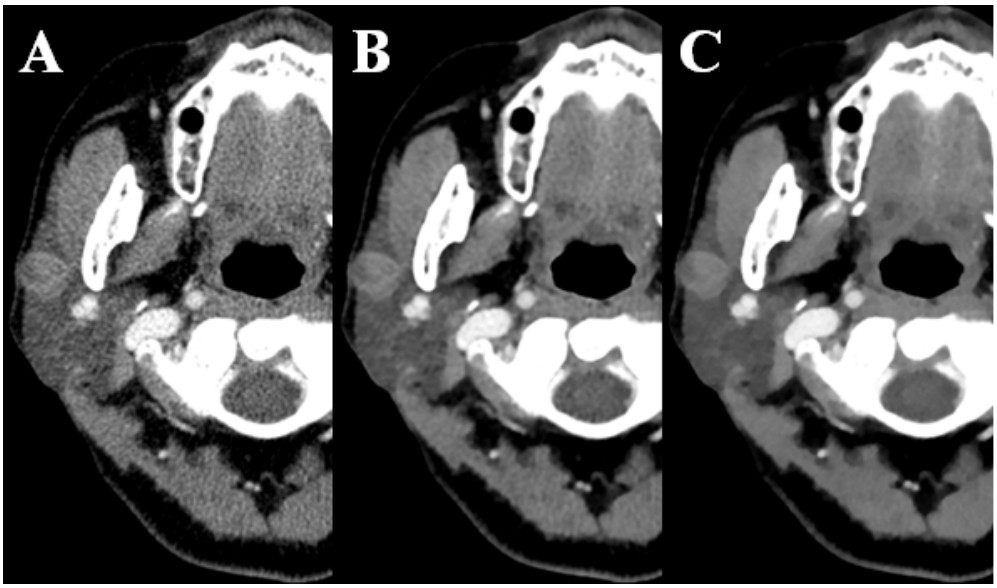

Figure 3. 45-year-old man with a right parotid gland mass.

Three axial image sets reconstructed using FBP (A), iDose^4 (B), and knowledge-based IMR (C) algorithms. Compared with those on the FBP- and iDose^4-reconstructed images, there is a significant decrease in the noise in the parotid region and significantly better contrast and characterization of the tumor on the iterative model-reconstructed image. The parotid tissue appears blotchy and pixelated on the iterative model-reconstructed image.

IV. DISCUSSION

In the present study, we evaluated the diagnostic utility of IMR for CT evaluations of palpable parotid gland masses. The study design included direct side-by-side comparisons of image noise and image quality with other reconstruction algorithms, namely FBP and iDose. Our results demonstrated that knowledge-based IMR yielded simultaneous, statistically significant objective and subjective improvements with regard to image quality and noise, and this finding was consistent with the results of previous studies [4-7].

Recently, several studies have reported the advantages of the IMR algorithm for CT evaluations of other body parts. We decided to assess the utility of this technique for parotid gland masses, because parotid gland imaging is susceptible to interference by streak artifacts from dental amalgam restorations that are frequently observed on CT images reconstructed with FBP algorithms[2]. Moreover, image contrast is another important parameter to assess the precise extent of the mass on CT, because the majority of parotid gland tumors are pleomorphic adenomas, which show poor contrast enhancement on CT images obtained 30 s after contrast administration and are difficult to detect against the background of parotid gland tissue[11].

Although the conventional FBP technique is the most widely used CT reconstruction algorithm because of the fast and efficient reconstruction, it can result in image deterioration due to systemic geometric distortion and streak artifacts with insufficient data collection[12]. With rapid advances in computer technologies, IR algorithms have been introduced as an innovative CT

reconstruction technique characterized by repeated modification processes with multiple iteration correction steps. This technique has resulted in a dramatic improvement in the overall image quality through noise reduction and adequate resolution[3,13]. IMR is the latest knowledge-based or model-based IR algorithm offered by Philips Healthcare. It optimizes the image reconstruction process by reflecting image and data statistics and systemic models. Therefore, the IMR algorithm requires a longer reconstruction time. However, we used the latest processors with greater computational capacity in the present study, which yielded an average reconstruction time of approximately 5 min only, which is acceptable for clinical use.

In the present study, we performed objective and subjective image analyses using several imaging parameters. Among the quantitative imaging parameters, CNR describes the extent by which differences between the attenuation from two different regions increase above the pixel-to-pixel variations[14]. Thus, CNR can be an excellent image quality parameter for the detection of low-contrast lesions. In the present study, CNR for IMR was excellent, and this will greatly aid in the detection and characterization of parotid masses, considering that different tumors with different cell types and enhancement patterns can develop in the parotid gland. In addition, in our subjective image analyses, we assessed artifacts and noise together because it is difficult to distinguish streak artifacts from noise, particularly in the region located between the mandible and temporal bone. We found that IMR resulted in significantly lesser overall noise and artifacts compared with the FBP and iDose[4] algorithms.

As reported previously, distinct image features noted on images reconstructed using IR techniques include a unique plastic texture and a blotchy, pixelated

appearance[15], which was significantly more prominent with IMR than with iDose[4] in the present study. Among the variety of image quality optimization methods applied in the IR process, the total variation minimization method has been widely used[16]. However, it inevitably results in oversmoothening of images because of its basic assumption. Therefore, a characteristic texture of CT images reconstructed using IR techniques may be observed in the form of oversmoothening in edge regions and a blotchy, pixelated appearance in nonedge regions[17]. Accordingly, to evaluate how the IMR algorithm affects the diagnostic performance of CT for parotid gland masses, we assessed a few qualitative image parameters such as delineation of the parotid mass and a blotchy, pixelated appearance in the present study. The average score for delineation of the parotid mass was significantly higher with IMR than with iDose[4] and FBP, probably because of significant noise reduction with the former. Moreover, the average scores for a blotchy, pixelated appearance as assigned by two readers was 3.76±0.76 and 4.02±0.68, respectively, for IMR, which were significantly lower than those for FBP and iDose4. However, the scores suggested that the blotchy, pixelated appearance may not affect or slightly affect the accurate diagnosis of parotid gland masses with IMR. Therefore, we believe that the unique image texture obtained with IMR will not influence the diagnostic performance in clinical practice, although the lack of awareness of radiologists with regard to this appearance remains a significant limitation of the IMR algorithm that can be overcome by increased experience and knowledge sharing.

Previous phantom studies have demonstrated that IMR enables a dose reduction of 60%-80% compared with FBP[18]. In the present study, the mean DLP for CT

performed at 100 kVp with the IMR algorithm was 149.22 ± 40.69 mGy-cm, and this was approximated to be 65% lower than the values previously obtained for CT performed at 120 kVp with the FBP algorithm at our institution. This indicates that IMR undoubtedly offer further radiation dose reduction compared with other reconstruction techniques, without severely compromising the image quality.

This study has several limitations. First, the image quality was analyzed on the basis of semiquantitative and qualitative parameters, and phantom experiments could have provided more accurate and detailed information about the image quality by using various physical metrics such as the modulation transfer function, section sensitivity profile, and noise power spectrum[19,20]. Second, although reviewers were blinded during subjective image analyses, they may have been able to distinguish the three image sets because of the unique image texture obtained with IMR. This could have led to assessment bias. Third, we could not compare diagnostic performance data (such as sensitivity and specificity) for the reconstruction algorithms because all patients had parotid gland masses. Finally, only 42 patients were included in the study, and future studies with larger sample sizes determined by statistical power analysis are necessary to further clarify our findings.

V. CONCLUSION

In conclusion, knowledge-based IMR is a feasible image reconstruction algorithm which can produce an excellent image quality and reduce image noise and artifacts for the evaluation of patients with parotid gland mass.

References

1. Lin C-C, Tsai M-H, Huang C-C, Hua C-H, Tseng H-C, Huang S-T. Parotid tumors: a 10-year experience. American journal of otolaryngology 2008;29:94-100.
2. Barrett JF, Keat N. Artifacts in CT: recognition and avoidance 1. Radiographics 2004;24:1679-91.
3. Geyer LL, Schoepf UJ, Meinel FG, Nance Jr JW, Bastarrika G, Leipsic JA, et al. State of the Art: Iterative CT Reconstruction Techniques. Radiology 2015;276:339-57.
4. Halpern EJ, Gingold EL, White H, Read K. Evaluation of coronary artery image quality with knowledge-based iterative model reconstruction. Academic radiology 2014;21:805-11.
5. Khawaja RDA, Singh S, Blake M, Harisinghani M, Choy G, Karosmangulu A, et al. Ultra-low dose abdominal MDCT: Using a knowledge-based Iterative Model Reconstruction technique for substantial dose reduction in a prospective clinical study. European journal of radiology 2015;84:2-10.
6. Park SB, Kim YS, Lee JB, Park HJ. Knowledge-based iterative model reconstruction (IMR) algorithm in ultralow-dose CT for evaluation of urolithiasis: evaluation of radiation dose reduction, image quality, and diagnostic performance. Abdominal imaging 2015;40:3137-46.
7. Ryu YJ, Choi YH, Cheon J-E, Ha S, Kim WS, Kim I-O. Knowledge-based iterative model reconstruction: comparative image quality and radiation dose with a pediatric computed tomography phantom. Pediatric radiology 2015:1-13.
8. Shrimpton P, Hillier M, Lewis M, Dunn M. National survey of doses from CT in the UK: 2003. The British journal of radiology 2014.
9. Jessen K, Panzer W, Shrimpton P, Bongartzm G, Geleijns J, Golding S, et al. EUR 16262: European guidelines on quality criteria for computed tomography. Luxembourg: Office for Official Publications of the European Communities 2000.
10. Landis JR, Koch GG. The measurement of observer agreement for categorical data. biometrics 1977:159-74.
11. Choi DS, Na DG, Byun HS, Ko YH, Kim CK, Cho JM, et al. Salivary Gland Tumors: Evaluation with Two-Phase Helical CT 1. Radiology 2000;214:231-6.
12. Shepp LA, Logan BF. The Fourier reconstruction of a head section. Nuclear Science, IEEE Transactions on 1974;21:21-43.
13. Seibert JA. Iterative reconstruction: how it works, how to apply it. Pediatric radiology 2014;44:431-9.
14. Hendrick RE. Breast MRI: fundamentals and technical aspects. Springer Science & Business Media; 2007.
15. Yasaka K, Katsura M, Akahane M, Sato J, Matsuda I, Ohtomo K. M

odel-based iterative reconstruction for reduction of radiation dose in a bdominopelvic CT: comparison to adaptive statistical iterative reconstr uction. SpringerPlus 2013;2:209.

16. Sidky EY, Pan X. Image reconstruction in circular cone-beam comput ed tomography by constrained, total-variation minimization. Physics in medicine and biology 2008;53:4777.
17. Qi H, Chen Z, Zhou L. CT Image Reconstruction from Sparse Projec tions Using Adaptive TpV Regularization. Computational and mathema tical methods in medicine 2015;2015.
18. Mehta D, Thompson R, Morton T, Dhanantwari A, Shefer E. Iterative model reconstruction: simultaneously lowered computed tomography r adiation dose and improved image quality. Med Phys Int J 2013;2:14 7-55.
19. Boone JM. Determination of the presampled MTF in computed tomog raphy. Medical Physics 2001;28:356-60.
20. Siewerdsen J, Cunningham I, Jaffray D. A framework for noise-power spectrum analysis of multidimensional images. Medical physics 2002; 29:2655-71.

ABSTRACT(IN KOREAN)

이하선 종괴 평가를 위한 조영증강 전산화단층촬영에서 knowledge-based iterative model reconstruction의 임상적 유용성 평가

연세대학교 대학원 의학과

김 기 욱

목적: 이하선 종괴의 전산화단층촬영 평가에서 knowledge-based iterative model reconstruction (IMR)의 임상적 유용성을 평가하고, filtered back projection (FBP)과 hybrid iterative reconstruction (iDose^4)의 소견과 비교한다.

대상 및 방법: 촉지가능한 이하선 종괴를 가진 42명의 환자를 대상으로, 조영증강 전산화단층촬영을 시행하였다. FBP, iDose^4 및 IMR을 사용하여, 동일한 형태의 영상을 재구성하였다. 배경잡음, 신호대잡음비 및 대조대잡음비를 포함한 정량적 영상지표를 측정하였다. 두 명의 영상의학과의사들이 5단계 평가 체계를 사용하여 잡음 및 인공물, 이하선 종괴 윤곽과 얼룩덜룩한 화소 모양에 대하여 주관적 평가를 시행하였다.

결과: IMR의 배경잡음은 다른 두 알고리듬의 배경잡음에 비하여 유의미하게 적게 측정되었으며 (p<0.001), IMR의 신호대잡음비와 대조대잡음비는 다른 두 알고리듬에서 측정된 값에 비하여 유의미하게 높게 측정되었다 (p<0.001). IMR은 다른 두 알고리듬에 비하여 유의미하게 적은 잡음 및 인공물을 보였고 더 뛰어난

이하선 종괴 윤곽의 영상 품질을 보였으나, 더 흔하게 얼룩덜룩한 화소 모양이 관찰되었다.

결론: IMR을 이용한 전산화단층촬영은 우수한 영상 품질과 감소된 잡음 및 인공물을 제공하여, 이하선 종괴의 평가에 유용하게 사용될 수 있다.

핵심되는 말 : knowledge-based iterative reconstruction, filtered back projection, 전산화단층촬영, 이하선 종괴